POLITECNICO DI TORINO
Repository ISTITUZIONALE

Coffee and turmeric bio-based shape-stabilized composite PCMs for thermal and solar energy storage applications

Original
Coffee and turmeric bio-based shape-stabilized composite PCMs for thermal and solar energy storage applications / Mishra, A.K., Morciano, M., Campagnoli, E., Giaretto, V., Fasano, M., Chiavazzo, E.. - In: SOLAR ENERGY MATERIALS AND SOLAR CELLS. - ISSN 0927-0248. - ELETTRONICO. - 297:(2026). [10.1016/j.solmat.2025.114136]

Availability:
This version is available at: 11583/3006341 since: 2026-01-08T11:59:50Z

Publisher:
Elsevier B.V.

Published
DOI:10.1016/j.solmat.2025.114136

Terms of use:

This article is made available under terms and conditions as specified in the corresponding bibliographic description in the repository

Publisher copyright

(Article begins on next page)

24 June 2026

Solar Energy Materials & Solar Cells 297 (2026) 114136

Contents lists available at ScienceDirect

Solar Energy Materials and Solar Cells

journal homepage: www.elsevier.com/locate/solmat

Coffee and turmeric bio-based shape-stabilized composite PCMs for thermal and solar energy storage applications

Amit Kumar Mishra [a], Matteo Morciano [a], Elena Campagnoli [a], Valter Giaretto [a], Matteo Fasano [a], Eliodoro Chiavazzo [a,b,*]

[a] Department of Energy, Politecnico di Torino, Corso Duca Degli Abruzzi 24, 10129, Torino, Italy
[b] Istituto Nazionale di Ricerca Metrologica, Strada Delle Cacce 91, 10135, Torino, Italy

ARTICLE INFO

Keywords:
Latent thermal energy storage
Ss-composite PCMs
Bio-based
Thermal conductivity enhancement
Power density
Thermal management
Photothermal conversion

ABSTRACT

Bio-based shape-stabilized composite phase change materials (ss-PCMs) are emerging as sustainable solutions for thermal and solar energy harvesting. However, typical shape-stability issues, poor thermal/optical properties, and complex synthesis methods hinder the use of such materials at large scale. This study reports the design of nanofiller-loaded bio-based composite PCMs with enhanced thermo-optical and mechanical properties (shape-stability). Incorporating a 25 wt% biomass-derived porous matrix (coffee/turmeric powder) significantly enhanced the material's structural integrity by effectively controlling PCM leakage while achieving a high latent thermal energy storage (TES) capacity of ~130 J/g. Graphene-loaded ss-composite PCMs demonstrated a significant photothermal conversion efficiency enhancement (106 %) and effective thermal management (TM) potential (superheat degree reduced by ~ 10 °C) compared to pristine PCM, due to the improved photo-thermal properties and power density. Thermal cycling (up to 500 cycles) and load-bearing capacity tests (~212,566 and ~31,242 N/m^2 across the phase transition zone) confirm the high reliability of the proposed novel ss-composite PCMs in terms of thermal and shape stability. These results highlight their strong potential for long-term TES applications, with stable performance even under adverse environmental conditions such as humidity and wetting. This research contributes to the design of bio-compatible (possibly edible) substance-based strategies for creating cost-effective composite PCMs with enhanced thermo-optical and shape stability characteristics, offering significant advancement for latent TES systems and TM technologies.

Nomenclature/Description/Unit

Symbol/ abbreviation	Description	Units
PCMs	Phase change materials	–
LA	Lauric acid	–
CBNP	Carbon black nanoparticles	–
GNP	Graphene nanoplatelets	–
SS	Shape stabilized	–
OCT	Optical coherence tomography	–
DSC	Differential scanning calorimetry	–
CSCPCM	Coffee-based ss-CBNP-loaded composite PCM	–
CSGPCM	Coffee-based ss-GNP-loaded composite PCM	–
TSCPCM	Turmeric-based ss-CBNP-loaded composite PCM	–
TSGPCM	Turmeric-based ss-GNP-loaded composite PCM	–
ΔH_s	Latent heat of the sample	J/g
c_p	specific heat capacity	J/(g K)
k_{pcm}	Thermal conductivity of pristine PCM	W/(m·K)
k_c	Thermal conductivity of nanocomposite PCM	W/(m·K)
k_{sc}	Thermal conductivity of ss-composite PCM	W/(m·K)
TC	Thermal conductivity	W/(m·K)
Ts	Interface temperature	°C
m_s	Mass of the sample	g
t	Time	sec.
A	Area	cm^2
I	Sunlight irradiance	mW/ cm^2
TES	Thermal energy storage	–
TM	Thermal management	–
q"	Heat load	W/cm^2
PTC	Photo-thermal conversion	–
η	PTC efficiency	%

* Corresponding author. Department of Energy, Politecnico di Torino, Corso Duca degli Abruzzi 24, 10129, Torino, Italy.
E-mail address: eliodoro.chiavazzo@polito.it (E. Chiavazzo).

https://doi.org/10.1016/j.solmat.2025.114136
Received 15 September 2025; Received in revised form 13 November 2025; Accepted 18 December 2025
0927-0248/© 2025 The Authors. Published by Elsevier B.V. This is an open access article under the CC BY license (http://creativecommons.org/licenses/by/4.0/).

1. Introduction

The rapid growth of human industrialization leads to a massive use of fossil fuels, releasing carbon dioxide, strengthening the greenhouse effect, and causing global climate issues [1,2]. As the global climate crisis grows more severe, scientists are increasingly focusing on sustainable and environmentally friendly energy materials [3]. However, the current advanced green energy technologies, such as solar cells/fuel cells technology, use toxic materials in their device's manufacturing and recycling processes can have long-term effects on the ecosystem [4,5]. Therefore, rising energy consumption and environmental concerns emphasize the development of sustainable energy storage and conversion technologies. Utilizing clean energy from the sun and waste heat has substantial potential to address environmental issues and energy shortages. Among the various approaches, thermal energy storage (TES) technologies stand out as an effective solution for balancing energy supply and demand while lowering carbon emissions [6–9].

In this aspect, photothermal conversion (PTC) energy storage strategies have attracted significant attention due to their cost-effectiveness and high efficiency [10–12]. On the other hand, the growing integration of electronic devices requires efficient thermal management (TM)/cooling technologies to prevent heat accumulation and ensure their safe/reliable function for long-term executions [13–16]. The application of thermal interface materials (TIMs) plays an essential role in enhancing heat dissipation efficiency and TM performance [17,18]. For heat storage/management and solar-thermal conversion, latent heat TES (LHTES) technology using phase change materials (PCMs) is an attractive choice due to their high energy density (nearly twice than sensible heat storage systems), low cost, and capability to store/release thermal energy isothermally during phase transition processes [19–22]. The TM of electronic devices is primarily achieved by active and passive cooling methods and currently, researchers are focused on designing smart passive cooling systems by employing shape-stabilized PCMs with integrated heat sink techniques, surpassing conventional PCM-based approaches [23,24].

For LHTES applications, lauric acid (LA) is a widely adopted organic PCM due to its solid-liquid phase change at relatively low temperature (~45 °C), non-corrosiveness, high TES capacity, no-phase-separation, no-supercooling, and good chemical/thermal stability [25,26]. These characteristics make LA an excellent candidate for various low-temperature PCM applications, including solar heat storage, buildings, waste heat recycling, electronics cooling, thermoelectric generators, and automotive fields [9,16,27,28]. Although LA shows outstanding performance in TES, the following major issues limit its practical suitability: (i) low heat conduction ability leading to slow charging/discharging rates, (ii) poor sunlight absorption thus low PTC efficiency, and (iii) risk of PCM leakage during melting phase transition [20,23,29–31]. These crucial drawbacks make conventional PCMs sub-optimal. Hence, shape-stabilized composite PCMs (also known as ss-composite PCMs or form-stable PCMs) are being developed to overcome the above obstacles. Generally, the inclusion of nanofillers with high thermal conductivity (TC) and shape-stabilization techniques such as microencapsulation, polymer matrix, and porous support material adsorption are employed to fabricate ss-composite PCMs with efficient thermophysical characteristics, compared to conventional PCMs [19,32]. Carbon-based nanofillers are particularly preferred due to their excellent optical and thermo-physical features, such as strong light absorption capacity, high heat conductivity, stable chemical activity, and low-density [33–36].

However, the preparation of ss-composite PCMs using the microencapsulation and polymer matrix techniques is time-consuming and costly due to complex synthesis steps like wet-chemical methods, polymerization, polycondensation, vacuum impregnation, participation of harmful/toxic precursors, limited TC, stability issues, etc., which greatly hinder their large-scale industrial production [37–40]. On the other hand, the porous support material adsorption technique has the advantages of its easy execution process, high efficiency, and low cost compared to the other ones [41,42]. The porous support, with its enhanced surface area and rich pore volume, generates capillary forces and surface tension that enable the retention of melted PCM within the porous skeleton, effectively preventing overflow [37,43].

Currently, the development of bio-based ss-composite PCMs with a porous structure from biomass is important for creating sustainable and efficient thermal/solar energy storage systems [29,44–46]. These support matrices derived from renewable/biomass resources have a prospect of being environment-friendly, minimizing toxicity, reducing carbon footprint, and achieving cost-effectiveness. To target all these characteristics including enhanced thermo-optical and structural properties, in the past many bio-based ss-composite PCMs were explored [17,40,41,45,47]. To achieve sustainable energy-saving solutions, it is beneficial to develop green ss-composite PCMs by integrating bio-based porous matrix additives that exhibit beneficial characteristics, including light absorption, high porosity, environmental sustainability, biodegradability, cost-effectiveness, chemical inertness, and antibacterial properties [48–52].

As found, the research work on bio-derived nano-enhanced PCM is still limited and faces scalability issues [53,54]. Previous studies have mainly focused on polymer-based or chemically synthesized ss-composite PCMs, which often require complex and time-consuming preparation processes and involve toxic or non-renewable precursors. Moreover, although several biomass-derived porous supports have been explored, the development of bio-based ss-composite PCMs that simultaneously ensure shape stability, enhanced thermo-optical performance, and simple synthesis remains a major challenge [55,56].

In this context, the present study reports the design of coffee- and turmeric-based nano-enhanced ss-composite PCMs incorporating CBNP and GNP fillers. These materials were prepared without the implication of any time-consuming or complex chemical processes, effectively overcoming the limitations of complex fabrication methods. The synergistic effect of the nanofillers and the bio-based porous matrices significantly improved heat transfer, light absorption, mechanical strength, solar-thermal conversion efficiency, and thermal stability compared to conventional PCMs.

This work therefore addresses the need for sustainable, scalable, and high-performance bio-based ss-composite PCMs for latent thermal energy storage and thermal management applications. The proposed materials exhibit high latent heat capacity (~130 J/g), enhanced photothermal conversion efficiency (~106 %), and excellent shape stability even under long-term cycling and load-bearing conditions, demonstrating their strong potential for large-scale, environmentally friendly TES and TM systems.

2. Materials and methods

2.1. Materials and bio-based ss-composite PCMs preparation

Lauric acid, used as base PCM, was purchased from Sigma-Aldrich (99 % purity), and the carbon black nanoparticles (CBNP) and graphene nanoplatelets (GNP) were purchased from PowderNano and Ossila Ltd., respectively, for improvement of heat conduction and photothermal conversion characteristics of pristine PCM. Turmeric powder (*Curcuma*) and coffee powder were used to prepare bio-based ss-composite PCMs. The above constituents received from the suppliers were used without any further purification and chemical treatments.

The CBNP and GNP-based nanocomposite PCMs were prepared by dispersing 4.0 wt% of respective nanofillers into the liquid LA, with the sample temperature maintained above the melting point (bath temperature kept at 50 °C). The mixture was then subjected to sonication in a water bath at ~53 kHz and full power for approximately 45 min. After incorporating 25 wt % coffee or turmeric powder into the 4 wt % CBNP-based colloidal solution, the resulting suspension was sonicated and stirred for 45 min. The resulting mixture was cooled at room

temperature and coffee-based ss-CBNP-loaded composite PCM (CSCPCM) or turmeric-based ss-CBNP-loaded composite PCM (TSCPCM) obtained. A similar sample preparation process was also used to prepare coffee-based ss-GNP-loaded composite PCM (CSGPCM) and turmeric-based ss-GNP-loaded composite PCM (TSGPCM), respectively. For thermophysical characterization, the investigated composite samples were prepared (diam. ~5.8 cm, height ~1.1 cm). Fig. 1 (a) shows the TEM image of the CBNP with discernible particle size of ~20 nm and Fig. 1(b)–(c) show TEM images of GNP indicating the planar structures and size of GNP flacks of ~1.5 μm. The nanofiller-loaded ss-composite PCMs preparation process steps are illustrated in Fig. 2. Tables 1 and 2 present materials' features and uncertainty-related information, respectively.

2.2. Characterization and performance evaluation of samples

The phase transition temperatures and latent heat values of the pristine LA and CBNP or GNP-loaded shape-stabilized composite PCMs were investigated by differential scanning calorimetry (DSC) under a nitrogen atmosphere with a 3 °C/min heating rate, using DSC 214 Polyma. The phase change characteristics and latent heat of pristine PCM and PCM-based ss-composites were obtained with an accuracy of ±0.2 %. The investigation of heat conduction characteristics (thermal conductivity/thermal diffusivity) of the PCM-based samples was determined using a Hot Disk Thermal Constants Analyzer (Hot Disk, TPS 500) with a nominal accuracy of ±5 % and ±10 %, respectively. The hot disk sensor comprises an electrically conducting pattern in the shape of a double spiral, which has been etched out of a thin metal (Nickel) foil. This sensor acts as a heat source for raising the PCM sample's temperature and concurrently recording the temperature changes with time. During measurements, a plane hot disk sensor is fitted between two pieces of the sample, and a small constant current is applied; the associated working principle/measurement details of the TPS 500 thermal analyzer are available in Ref. [57]. Optical coherence tomography (OCT) was used to study the microscopic features of the designed ss-composite PCMs using Thorlabs Ganymede (Fig. 4); load-bearing tests were carried out applying a calibrated mass of 6.5 kg on the PCM-based samples (dimensions: 30 mm × 10 mm × 6 mm, mass 2.8 g) and then assessing their shape-stability after several thermal cycles across the phase transition zone. The investigation of the thermal stability of PCM-based samples was done with thermogravimetric analysis (TGA) by using TG 209 F3 Tarsus (test range: 25–350 °C, rate: 5 °C/min, N_2).

A solar simulator (infinityPV ISOSun) was used to mimic concentrated solar light (150 mW/cm^2) and assess the PTC performance of ss-composites PCMs: the sample's temperature variation was recorded by k-type thermocouples every second. The thermal management performance of the ss-composite PCMs, compared to pristine PCMs, was evaluated by monitoring the variation in interface temperature (Ts) between the Al-plate (2 mm thick) and the incorporated sample (1 mm thick) under a constant heat flux of 0.28 W/cm^2. Each measurement was performed 3 times and the mean value reported along with the standard deviation.

3. Results and discussion

3.1. Phase change characteristics

Fig. 3(a) and (b) show the heat flow curves, during melting and solidification for the pristine PCM and coffee/turmeric-based ss-composite PCMs, respectively. The heat flow curves exhibit a single endothermic peak (energy absorbed) or exothermic peak (energy released), indicating first-order solid-liquid phase transitions. The latent heat values of the respective samples were determined from the areas under the heat flow curves. DSC revealed the peak melting and solidification temperatures of pristine PCM as 45.9 °C and 40.1 °C, respectively. The latent heat of pristine PCM during melting/solidification phase transition processes amounted to ~172.5 and ~170.4 J/g, respectively. The latter values find good agreement with previously reported results in the literature [58,59]. It is evident from Table 3 that the phase transition temperatures of ss-composite PCMs were not altered substantially with the presence of additives (shape-stabilizer agents: coffee/turmeric powder; nanofillers: CBNP/GNP), which illustrates the absence of any effective interaction between the incorporated additives and the PCM base material. DSC analysis (Fig. 3-c) reveals that the latent heat value and specific heat capacity of the designed ss-composite PCMs are lower than pure PCMs, coherently with previous evidence in the literature [60–62]. Despite this, the bio-based ss-composite PCMs achieved a high latent heat value of approximately 130 J/g, with a decrease of about 25 % compared to the latent heat of pure PCM. Nevertheless, they still demonstrate significant potential for TES capacity in industrial applications. In the solid state, the examined c_p value of ~2.03 J/(g · K) for LA shows good agreement with literature data at room temperature [63].

The lower latent heat and specific heat capacity of ss-composite PCMs with respect to the bare PCM is attributed to the effective reduction of PCM mass content within the composite core volume, since additives like coffee/turmeric powder are inert and do not show phase transition thus not being able to contribute by latent heat storage, and CBNP/GNP have poor c_p compared to the host matrix [64–67]. An overview of the measured phase change characteristics and specific heat capacity of the tested PCM-based samples is reported in Table 3.

Optical coherence tomography (OCT) is a contactless and non-destructive technique for high-resolution microstructure imaging within scattering media based on depth-resolved optical reflectivity [68,69]. Fig. 4 (a) and (c) show the OCT images of the prepared ss-PCMs (TSPCM and CSPCM), while Fig. 4(b)–(d) show their front reflection images, respectively. These OCT images illustrate the internal microstructure of ss-PCMs, identifying distinct components with brighter and darker streaks, which correspond to the pristine PCM and supporting matrix (turmeric/coffee) uniformity distributed within the composite. These OCT microstructural features helped to analyse the homogenous

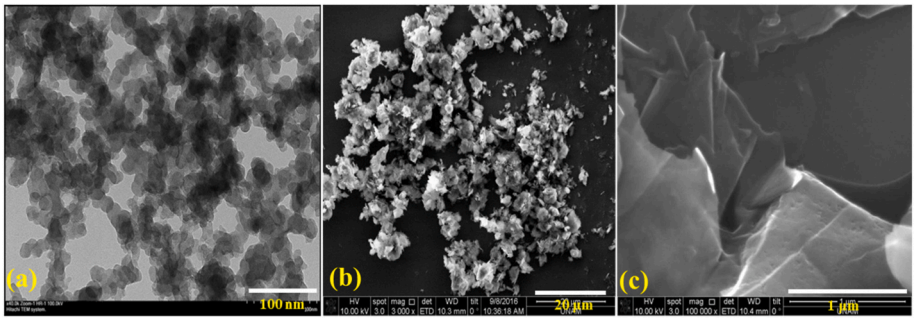

Fig. 1. TEM images of (a) carbon black nanoparticles (CBNP), (b)–(c) graphene nanoplatelets (GNP), which are provided by PowderNano and Ossila Ltd., respectively.

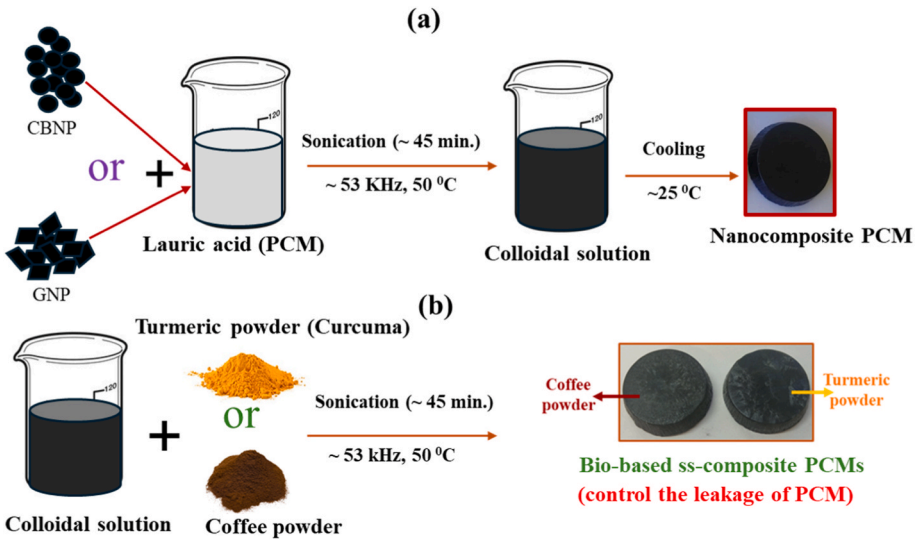

Fig. 2. Illustration of (a) CBNP and GNP-based nanocomposite PCMs; (b) coffee/turmeric-based ss-composite PCMs preparation steps.

Table 1
Description of materials' suppliers and features.

Material	Source	Purity (%)	Dimensions	Specific surface area (m^2/g)	Bulk thermal conductivity (W/m·K)
Lauric acid (LA)	Sigma-Aldrich	~99	–	–	~0.20
Carbon black nanoparticles (CBNP)	Powder-Nano	~98	Size ~20 nm	~195	~0.2–0.4
Graphene nanoplatelets (GNP)	Ossila Ltd.	~99.9	Size ~1.5 μm, Thickness ~3 nm	~800	~3000
Coffee powder	Nescafe Classic	~100	–	–	~0.11–0.13
Turmeric powder	TRS Asia's Finest Foods	~100	–	–	~0.07

Table 2
Uncertainty of instruments/tools.

Instruments/tools	Model	Property/quantity	Uncertainty
Hot Disk Thermal	TPS500	Thermal conductivity	~ ± 5 %
Differential scanning calorimetry (DSC)	DSC 214 Polyma	Phase change temperatures and latent heat values	~ ± 0.2 %
Solar simulator	infinityPV ISOSun	Solar irradiance	~ ± 2 %
Thermocouple	K-type	Temperature measurement	~ ± 1.5 °C
Heat pad	RS PRO silicon heater	Thermal load	~ ± 5 %

Table 3
DSC analysis of ss-composite PCMs.

Sample	Melting Process		Solidification Process		
	Melting point (°C) (±0.1 °C)	Latent heat (J/g) (±0.4 J/g)	Freezing point (°C) (±0.1 °C)	Latent heat (J/g) (±0.4 J/g)	c_p (J/(g K)) Solid-state, 25 °C
PCM (LA)	45.9	172.5	40.1	170.4	2.03
CSCPCM	46.2	133.7	39.2	130.5	1.94
CSGPCM	46.7	126.0	39.9	122.8	1.86
TSCPCM	46.3	134.1	39.5	127.4	1.85
TSGPCM	46.5	142.0	39.6	133.2	1.72

distribution of the PCM within the supporting matrix and reveal that their present porous activity characteristics contribute to improving the structural integrity of the ss-composite PCMs.

4. Enhanced heat conduction performance

Fig. 5(a) shows the enhancement of TC of lauric acid-based nanocomposite PCMs compared to pristine PCMs. Thermal measurement results show that the TC of pure PCM is effectively enhanced with the inclusion of these carbon-based nanofillers. The TC enhancement (%) was calculated using the expression $\left[\left(k_{c/sc}/k_{pcm} - 1\right)*100\right]$, where k_c, k_{sc}, and k_{pcm} indicate the effective TC of the nanocomposite PCM, ss-composite PCM, and pristine PCM in the solid state, respectively. The TC of solid pristine PCM was enhanced by ~50 % and ~75 % after 4 wt % CBNB and GNP loading of nanoparticles, respectively. This is attributed to the generation of internal stress fields during solidification [70,71]; the dispersed nanoparticles in the solution are therefore pushed towards the grain boundaries and build efficient heat conduction pathways (percolation networks) [72–74]. The superior TC enhancement of GNP-loaded nanocomposite PCMs could be attributed to its inherent higher bulk TC (~3000 W/(m · K)) and to the 2D structure of nanoparticles that ease plane-to-plane contacts, which comparatively help to create efficient percolation pathways with lower thermal resistance [75,76]. On the other hand, CBNP (expected bulk TC ~ 0.25–4.0 W/(m · K)) is substantially poorer than GNP also work to effectively enhanced the TC of pristine PCM is attributed due to their high compressibility, and volume-filling characteristics, leading to form quasi-2D percolation networks in the solid state [19,77]. Fig. 5 (b) illustrates schematically the nanofiller percolation networks created

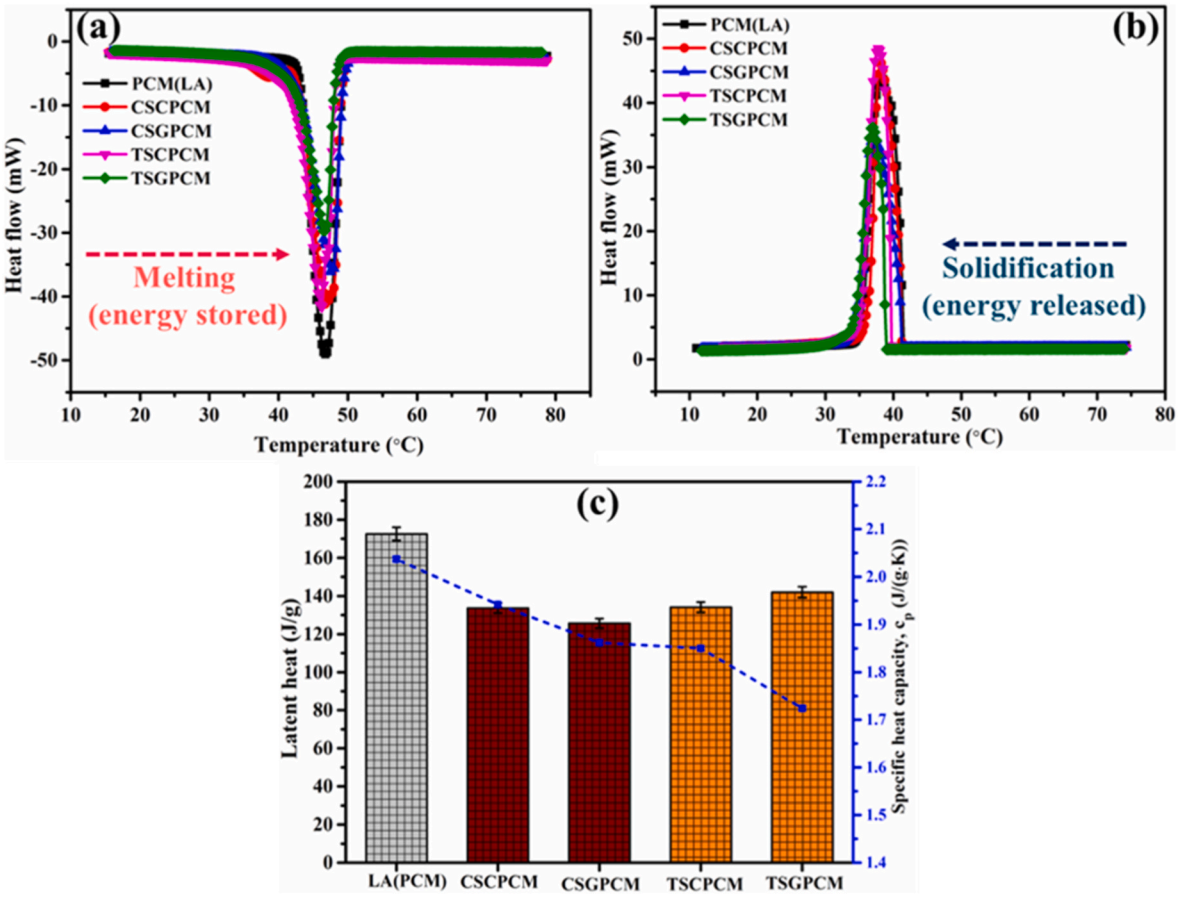

Fig. 3. (a)–(b) shows DSC curves during the melting and solidification processes of various coffee and turmeric-based ss-composite PCMs. (c) Variation of latent heat values during melting, and specific heat capacity of respective ss-composite PCMs at 25 °C. Phase change characteristics of pure PCM are also shown for comparison.

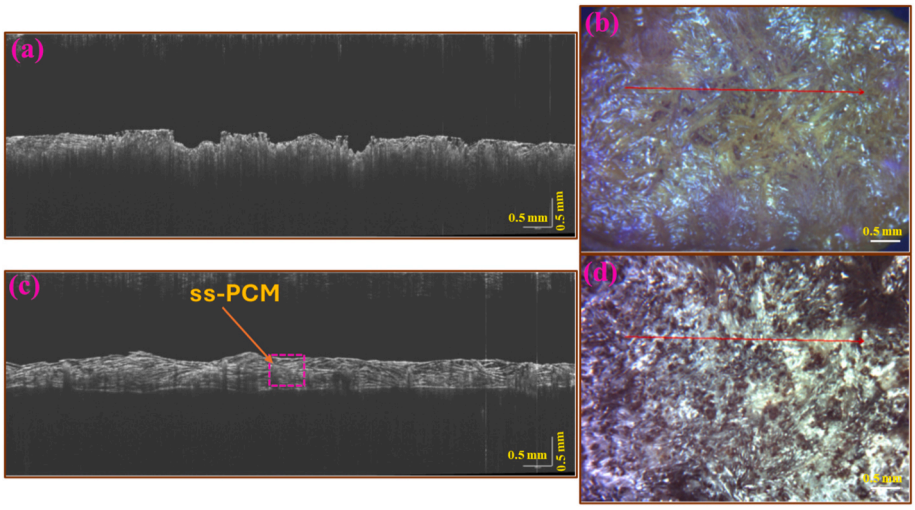

Fig. 4. (a) and (c) show OCT images of turmeric and coffee-based shape-stabilized PCMs. (b) and (d) show their corresponding front reflection images, respectively. The scale bars for lateral/axial dimensions refer to 0.5 mm.

during the solidification of the host matrix, which improves phonon-mediated heat transfer in the solid state.

In Fig. 5 (c), coffee and turmeric-based ss-composite PCMs show enhanced TC with respect to pristine PCM, however, the achieved TC is lower than their respective CBNP and GNP nanocomposite PCMs (without shape-stabilization). This is because the considered supporting matrixes (coffee/turmeric powder) have poor heat conduction characteristics (lower than bare PCM) [67,78,79]. On the other hand, ss-composite PCMs achieved better heat transfer efficiency than pristine PCMs due to the contribution of the nanofiller's thermophysical properties and well-stabilized network pathways (facilitating the phonon propagation within the composite matrix) [23,80]. The investigated thermal properties of ss-composite materials are summarized in Table 4.

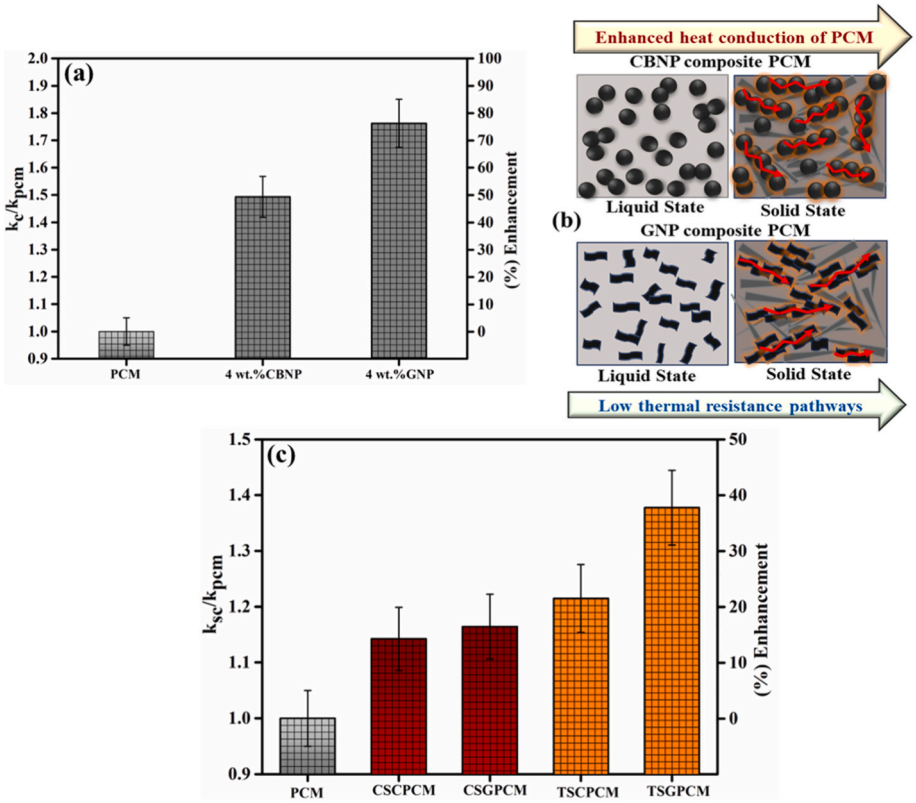

Fig. 5. (a) Variation of k_c/k_{pcm} and related % enhancement for PCM at 4 wt% CBNP and GNP loadings. (b) Schematic representation of percolating network pathways enhancing heat transfer in composite PCMs. (c) Variation of k_{sc}/k_{pcm} and related % enhancement for coffee and turmeric-based ss-composite PCMs. k_c, k_{sc} and k_{pcm} indicate the effective TC of the nanocomposite PCM, ss-composite PCM, and pristine PCM in the solid state, respectively.

Table 4
Thermal properties of all investigated samples.

Samples	Thermal conductivity (TC) (W/(m·K)) (±5 %)	Thermal diffusivity (mm^2/s) (±10 %)	TC (%) enhancement/ respect to pure PCM
LA (PCM)	0.219	0.102	0
4 wt% CBNP	0.327	0.222	49.3
4 wt% GNP	0.385	0.255	75.8
CSCPCM	0.250	0.146	14.3
CSGPCM	0.255	0.189	16.4
TSCPCM	0.265	0.165	21.0
TSGPCM	0.301	0.205	37.4

4.1. Improved shape-stability of PCM

The shape-stability assessment of pristine PCM and its corresponding coffee/turmeric-based ss-PCMs was evaluated as a function of time under constant load-bearing pressure stress (~212.6 kN/m^2). As illustrated in Fig. 6 (a), the bare PCM fails to maintain its structural integrity within a brief period (20 min). Instead, the coffee/turmeric-based ss-PCMs demonstrated significant structural integrity performance for over 20 h at room temperature. This indicates that the proposed coffee/turmeric-based ss-PCMs have enough mechanical strength to avoid liquid PCM leakage/cracking in engineering applications. Furthermore, the material leakage test was also carried out at phase transition (~45 °C). The pristine and ss-composite PCMs were placed on a hot plate maintained at ~50 °C: Fig. 6 (b) (I-VI) shows pure PCM and ss-composite PCMs (CSCPCM and TSGPCM) during heating at time t = 0 to up to 300 s across the phase transition zone. It can be seen from Fig. 6 (b) (IV) that significant leakage is observed in the case of pristine PCM, whereas material leakage is effectively controlled for the ss-composite PCMs cases (V-VI). Furthermore, the shape-stability/leakage test of CSCPCM was checked against applied compressed force through a weight of 1000 g (~31.2 kN/m^2) (Fig. 6 (c)). It was observed that such bio-based supporting matrices effectively maintained structural integrity, even under mechanical stress at temperatures exceeding the melting point (Table 5). The above results reveal that coffee and turmeric support have substantial potential to improve shape-stability and mechanical strength. Their distinct material characteristics related to the improvement of light-harvesting and microstructural properties have been previously explored [48,81–83], however, the sustainability of such cost-effective composite PCMs along with their synergic contribution with nanostructure characteristics in terms of thermo-optical and thermal management, still needs further exploration. The superior-weight load (stress) bearing characteristics across the phase transition zone reveal their high practical suitability for TES applications.

4.2. Photothermal conversion performance

Fig. 7(a) shows a schematic diagram of the PTC performance investigation. The PTC performance of ss-composite PCM in comparison to pristine PCM was evaluated under simulated sunlight irradiation at an intensity of 150 mW/cm^2, therefore mimicking concentrated solar energy. Fig. 7 (b) shows a schematic presentation of the basic mechanism of the PTC process: the incorporated nanofillers are rich in π-conjugated electrons, which absorb radiant energy and are then excited from π bonding to π* antibonding molecular orbitals. After that, excited electrons return to the lower state through lattice relaxation, and a portion of stored radiant energy is converted into heat [87]. Fig. 7(c) displays the temperature variation of different ss-composite PCMs irradiated by such a light source, which were recorded by DAQ system. Intense solar irradiation causes the temperature of ss-composite PCMs to rise rapidly,

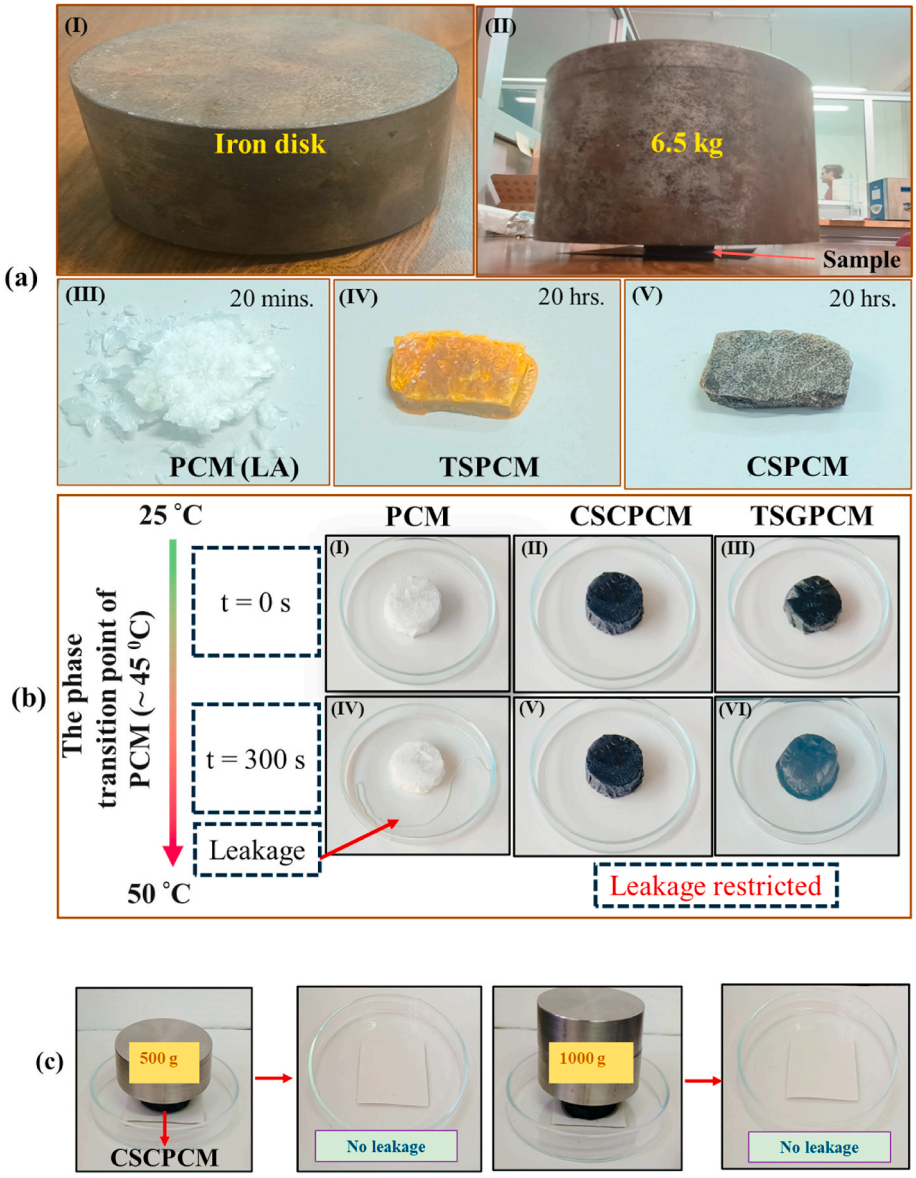

Fig. 6. (a) Investigation of shape-stability test between pristine PCM and coffee/turmeric ss-PCMs (dimensions: 30 mm × 10 mm × 6 mm) under a pressure exerted by 6.5 kg weight (at 25 °C). (b) Typical photographs of the pristine PCM, coffee/turmeric-based ss-composite PCMs across their phase transition temperature. (c) The shape-stability was investigated via leakage test for CSCPCM (radius: 10 mm; height: 10 mm) against compressed loading weights of 500 g or 1000 g at 50 °C.

Table 5
Comparison of the load compression test of the designed ss-composite PCMs with the previous studies.

Sample	Load bear capacity (Compression)	Area (cm^2)	Ref.
PEG-CNC	50 g	–	[84]
LA@CHNP	180 g	7.06	[85]
PCLS-4	200 g	4.00	[86]
CSCPCM	1000 g	3.14	Present study

unlike pure PCMs. Additionally, in the phase transition region, the temperature stabilizes on a plateau value, namely the melting temperature. When the power was turned off, the temperature dropped dramatically and led to the solidification phase at constant temperature during phase change. The experimental findings show that ss-composite PCMs have better PTC performance than PCMs. This could be attributed to the presence of carbon nanofillers (CBNP and GNP), which act as strong light absorbers and converters into heat. This behaviour is coherent with previous studies, which demonstrated that carbon-based nanofillers like CNTs, GNPs, and EG (expanded graphite) have superior optical absorption in the solar spectrum compared to conventional PCMs. This is due to the resonant π-plasmon excitation/band-to-band transitions under solar radiation [35,88], which leads to an increased extinction coefficient up to ~ 0.6 cm^{-1} [19,34,89]. Moreover, the incorporated coffee/turmeric shape-stabilizers also has light absorption characteristics due to melanoidin's pigment and curcumin structure, which synergically contribute with nanofillers to boost the PTC conversion performance of their respective ss-composite PCMs [90–94].

The PTC efficiency (η) is defined as the ratio of the TES during the solid-liquid phase change process to the incident light energy, evaluated as:

$$\eta = \frac{m_s \Delta H_s}{IA(t_e - t_s)}, \quad (1)$$

where ΔH_s, m_s, I, A, and $(t_e - t_s)$ indicate latent heat, mass of the sample, sunlight irradiance, sample area, and phase transition interval (t_e and t_s indicating transition ends/starts time), which are determined by the

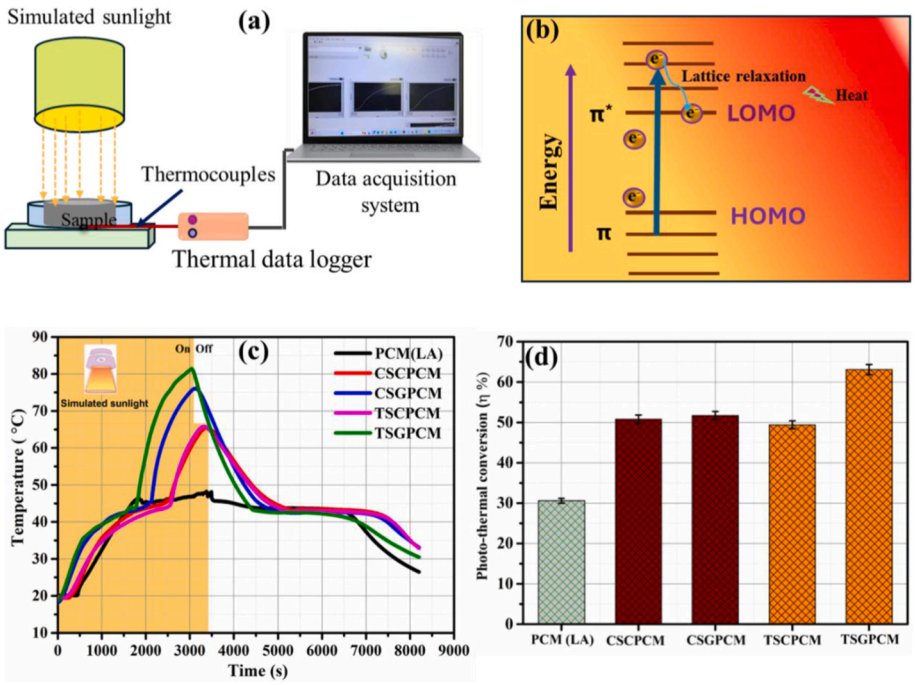

Fig. 7. (a)–(b) Schematic representation of photo-thermal measurement setup and PTC and storage mechanism. (c) Photo-thermal conversion for pristine PCM and coffee/turmeric-based ss-composite PCMs. (d) Investigated PTC efficiency of samples.

tangent method at the phase transition zone of the temperature change curves (intersection of pre and post transition tangent with phase transition (plateau) region [95], respectively. It can be seen from Fig. 7 (d) that the PTC efficiency of ss-composite PCMs was evaluated in comparison to pristine LA, resulting in 30.6 %, 50.8 %, 51.7 %, 49.4 %, and 63.1 % for PCM, CSCPCM, CSGPCM, and TSCPCM, respectively. The ss-composite PCMs show high PTC performance on account of their enhanced light absorption capacity in the UV–Vis–NIR frequencies and effective heat diffusion performance within the host matrix. The TSGPCM shows better PTC performance compared to other PCM-based ss-composites (Fig. 7 (d)): this could be attributed to better heat conduction (Fig. 5 (c)), which comparatively accelerates the LHTES charging process. The parameters related to the calculation of PTC efficiency are listed in Table 6. We also compared the effective enhancement of the photo-thermal efficiency of the proposed bio-composite PCM relative to its host matrix (PCM) with previously reported bio-based and conventional composite PCM enhancements (see Table 7). In summary, the designed composite PCMs have high TES capacity (latent heat) and solar-thermal conversion ability (photo-thermal efficiency).

4.3. Stability and durability assessment

The thermal stability of PCM-based samples is a crucial parameter for their application in real-world applications: to assess it, TGA experiments were carried out. The TGA temperature increment range was set between 25 and 350 °C at a heating rate of 5 °C/min. Fig. 8 (a) shows the weight loss (W, in %) as a function of sample temperature (T) for the pristine LA and its coffee and turmeric-based ss-composite PCMs (CSCPCM and TSGPCM). All materials show a constant and smooth trend up to 110 °C, thereafter decomposition has started. Up to ~100 % and ~75 % decomposition (weight loss) occurred for the pristine and ss-composite PCMs cases, respectively, just below ~ 240 °C. Fig. 8 (b) shows the variation of differential weight (dW/dT, differential thermal analysis – DTA) as a function of sample temperature for the pristine LA and respective ss-composite PCMs. Single peaks dW/dT curves indicate one-step thermal degradation at ~235, ~227, and ~225 °C for the pristine PCM, CSCPCM, and TSGPCM, respectively. Beyond, 240 °C, the bare PCM was completely decomposed (i.e. evaporated) and the residual weights (25 wt%) corresponded to the residual coffee/turmeric matrixes. The TGA and DTA findings reveal that LA and designed ss-composite PCMs exhibit similar thermal characteristics and have excellent thermal stability within the operating range for low-temperature TES applications, namely below 110 °C.

The assessment of thermal stability performance (after several melting/solidification cycles) of ss-composite PCMs is essential for practical TES applications in the long term. To probe the thermal stability of the ss-PCMs in comparison to pristine PCMs, DSC studies were conducted over 500 successive melting and cooling thermal cycles for each sample. Fig. 9(a–b) shows the DSC heat flow curves during repeated (heating/cooling) cycles of PCM-based samples. Even after (500 cycles), the phase transition temperatures and latent heat values of samples remain almost unchanged. Again, the shape-stability (leakage-test) of shape-stabilized PCMs was investigated by performing 100 melting/solidification thermal cycles across a temperature range (25–50 °C) using (forced ventilation oven), and mass loss occurred only

Table 6
Photothermal conversion-related parameters of the samples.

Sample	m_s (g)	t_s (sec)	t_e (sec)	(t_s- t_e) (sec)	ΔH_s (J/g)	A (cm^2)	I (mW/cm^2)	η (%)
PCM(LA)	32	1775	3465	1690	172.5	71	150	30.6
CSCPCM	32	1650	2440	790	133.7	71	150	50.8
CSGPCM	32	1368	2100	730	126.0	71	150	51.7
TSCPCM	32	1721	2535	814	134.1	71	150	49.4
TSGPCM	32	1112	1762	650	137.6	71	150	63.1

Table 7
Comparison of PTC enhancement of bio-based composite PCMs with other reported bio-derived and conventional composite PCMs in related research.

Sample	ΔH_m (J/g)	η (%) enhancement of composite PCM in comparison to host PCM matrix	Light Intensity (mW/cm^2)	Preparation of sample process (complexity)	Ref.
LA/EG-5 %	154.5	34.78	100	complex	[96]
CSC/PEG/GF10	123.6	162.24	150	complex	[97]
CF/LA-MA/BN35 %	95.05	100	150	complex	[98]
PEG/BPC@M	154.9	47.22	120	complex	[99]
GO3/PEG	84.27	87.3	100	simple	[100]
70 % EG/OP70	126.7	68.20	–	simple	[101]
CW-3/OP44E	206.3	50	100	complex	[102]
PCS600	100.2	54.49	100	complex	[103]
CSGPCM	126.0,	68.95,	150	Very economical and simple	**Present study**
TSGPCM	142.0	106.20	150		

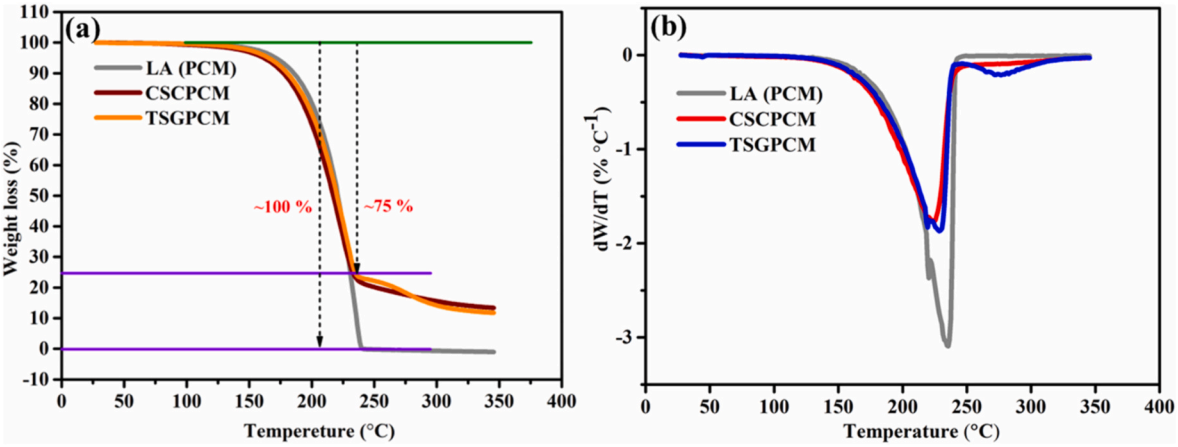

Fig. 8. (a) TGA and (b) DTA curves of pristine PCM (LA) and CSCPCM/TSGPCM ss-composite PCMs, respectively.

1.78 and 5.14 wt%, respectively, reveal their practical potential for TES coherently with earlier studies [45,48]. The typical photographic images and minimal mass loss reveal these bio-based ss-PCMs have superior leakage control activity (Fig. 9c–d). Furthermore, the durability of the heat conduction performance of their ss-composite PCMs was also analysed after prolonged 100 phase change cycles. These findings reveal the thermophysical characteristics of designed ss-composite PCMs sustained superior reliability, which shows their potential for sustainable TES and TM applications (Fig. 9-e).

Furthermore, for real-world practical applications (the effect of moisture/humidity on ss-composite PCMs' thermal characteristics is interesting to explore) the thermal stability of designed ss-composite PCMs also demonstrated underwater by carrying out successive melting/cooling cycles across its phase transition temperature with the help of a temperature management furnace. It can be noticed from (Fig. 10-c) that after going through multiple phase change cycles (100 times) the DSC thermal characteristics of these ss-composite PCMs remain unchanged (latent heat ~ 125 J/g; closed to original cases), which reveals their practical suitability against moisture and high potential to sustain and perform in different thermal environments.

4.4. Thermal management performance

Executing effective thermal regulation and management for electronic devices utilizing PCM-based passive techniques remains a current area of interest [16,104,105]. Fig. 11(a) shows a schematic illustration of the experimental setup for investigating the thermal management performance of ss-composite PCMs compared to pristine PCMs. To reveal their TM ability, the variation of interface temperature (T_s) characteristics of pristine PCM and different ss-composite PCMs were recorded during the melting process. A constant uniform heat load (flux) (q" = 0.28 W/cm^2) was supplied by a heater pad (RS pro silicon heater) connecting a DC power controller. The temperature variation characteristics at the interface between the Al plate (thickness: 2 mm) and PCM-based sample (thickness: 1 mm) were recorded using (k-type) thermocouples. Experimental findings from Fig. 11(b) show the variation in interface temperature (T_s) for Al plate - pristine PCM and Al plate - ss-composite PCMs cases, which underwent distinct behavior compared to bare Al plate - air (without PCM). This is attributed to PCM having high latent TES ability across its phase transition region and being helpful in effective heat storage/thermal management. Furthermore, findings reveal that TM performance is significantly enhanced due to the employment of ss-composite PCMs, since a more stable temperature control and superheat degree minimized by approximately 10 °C (indicated by purple arrow, Fig. 11-b). The thermal cycling performance reveals that the TM activity (blue region: effective heat storage/TM control) of the designed ss-composite PCMs is quite durable (across phase transition zone) and suitable for long-term TM applications (Fig. 11-c). The TM characteristics of our designed bio-based ss-composite PCMs highlight their efficacy in TM fields as resuming the earlier demonstrated ss-composite PCM's TM performance in BTMS applications [23,106–109]. This is attributed to the designed nano-enhanced ss-composite PCMs, which have high heat conduction and power density, significantly boosting the TM capacity, especially for applications involving electronic components and batteries.

5. Conclusion

In the present work, coffee/turmeric bio-based ss-composite PCMs are designed to the demand for effective and sustainable solutions for TES and management. The synergic contribution of nanofillers (CBNP/GNP) with supporting matrix (coffee/turmeric) characteristics boost the

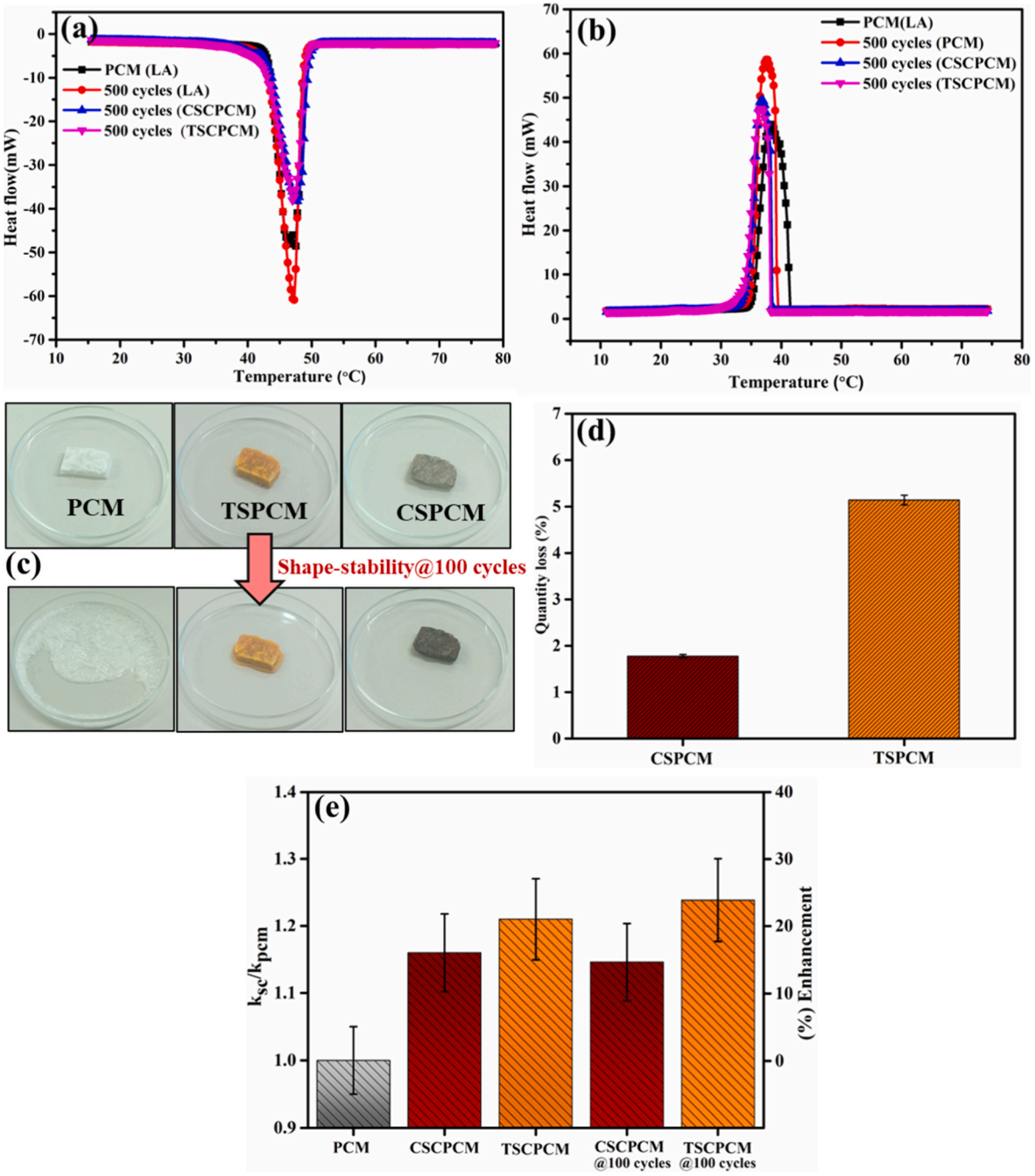

Fig. 9. (a)–(b) Heat flow curves during melting/cooling of pristine PCM and coffee/turmeric-basedss-composite PCMs. (c) Shape-stability performance of ss-composite PCMs by repeated thermal cycles across their phase transition temperature. (d) Evaluated sample's mass loss (%) after 100 cycles. (e) Durability of thermal conduction characteristics of ss-composite PCMs after 100 cycles.

thermo-optical, and mechanical properties of pristine PCM. The experimental findings demonstrate that nano-enhanced ss-composite achieved high PTC efficiency enhancement (~106.28 %) and structural integrity by preventing PCM leakage across the phase transition zone. This is attributed to GNP and CBNP nanofillers exhibiting strong light absorption characteristics and improved heat dissipation performance within composite through their conductive pathways. The porous characteristics of coffee and turmeric power effectively minimized the mass loss (<5 %) after ~100 thermal cycles, demonstrating their excellent shape stability, this stability is attributed to capillary forces and surface tension activity between the ss-porous matrix and PCM. The designed ss-composites show a high TES density (latent heat value) of approximately 130 J/g across the phase transition zone. The thermal cycles testing reveals the designed ss-composite PCMs have high thermal stability and LHTES performance. The ss-composite PCMs show superior TM activity (minimizing the superheat degree by ~ 10 °C) and their durable thermal features encourage their execution for long-term applications. The designed low-cost and biodegradable nano-enhanced ss-composite PCMs exhibit high thermo-optical characteristics and shape stability, making them suitable for sustainable energy storage and conversion. As cost-effective bio-composite materials, they have the potential to play a significant role in low-temperature energy storage (LHTES) applications, including thermal regulation of buildings, electronics cooling, solar-thermal systems, textiles/wearables, and battery thermal management. Despite such advancement of bio-based composite PCMs for effective TES and solar-thermal conversion. The future

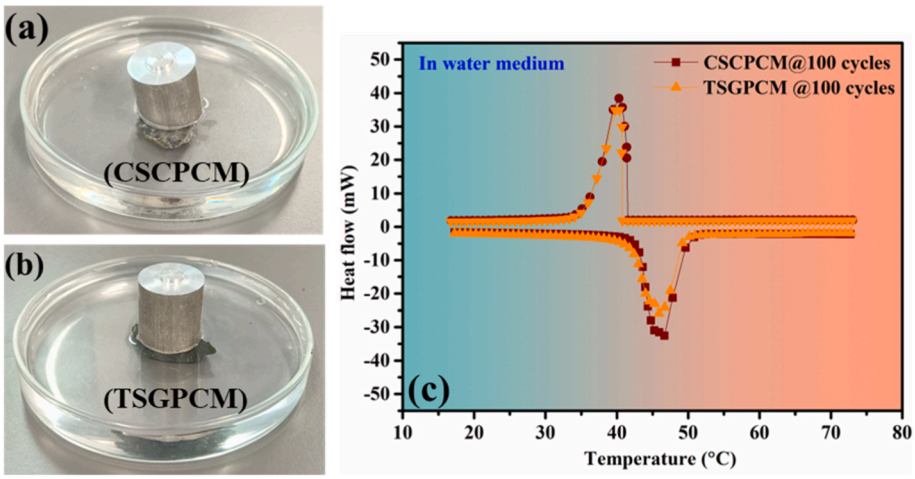

Fig. 10. **(a)–(b)** show the typical photographic images of CSCPCM and TSGPCM ss-composite PCMs that went through 100 thermal cycles (melting/solidification) underwater; (c) DSC curves of respective ss-composite PCMs after completion of 100 thermal cycles.

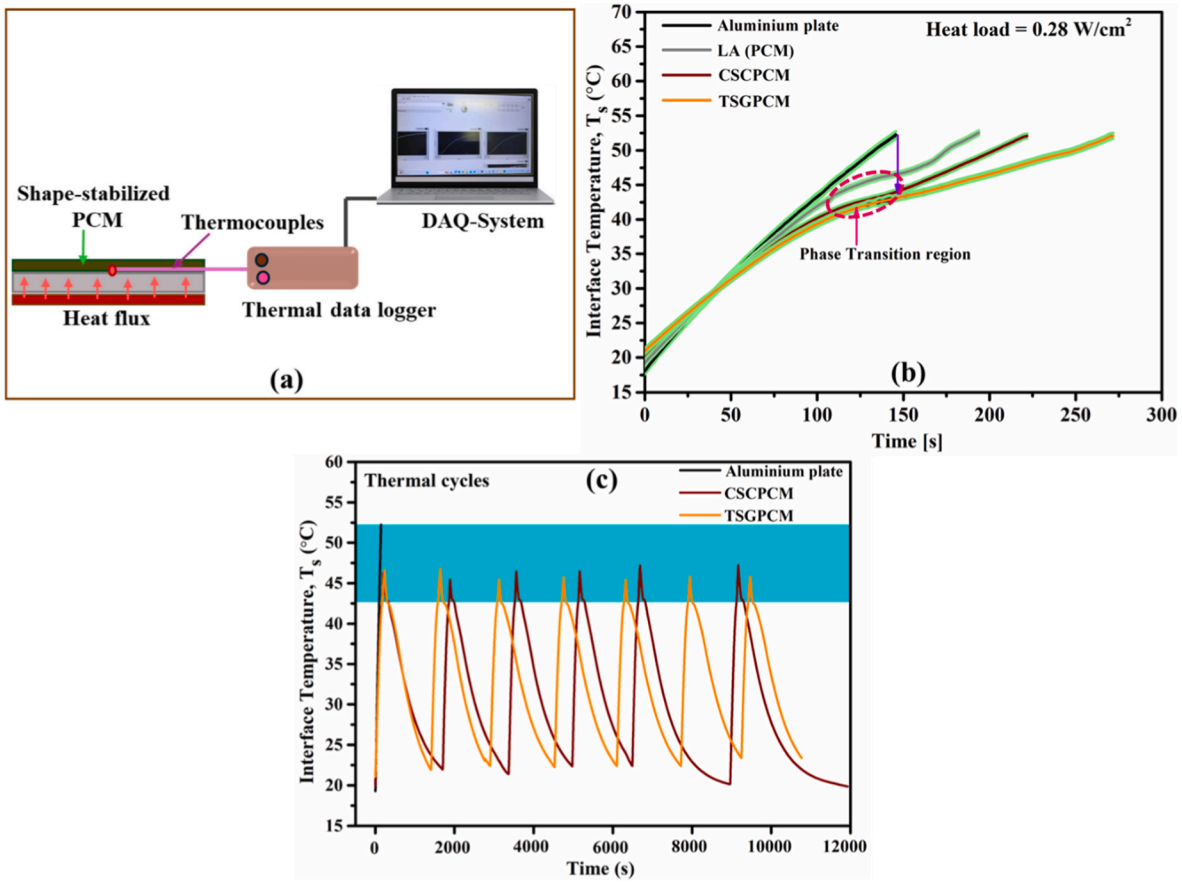

Fig. 11. **(a)** Schematic of thermal measurement performance setup; (b) Temperature evolution of pristine PCM and Coffee/Turmeric-based ss-composite PCMs; (c) Investigated the TM activity of ss-composite PCMs by performing thermal cycles. The error band (green trace) represents the possible measurement uncertainty. (For interpretation of the references to colour in this figure legend, the reader is referred to the Web version of this article.)

research should focus on optimization of additive concentration, long-term thermal/chemical stability, and testing their TES performances under field operation.

CRediT authorship contribution statement

Amit Kumar Mishra: Writing – original draft, Visualization, Methodology, Investigation, Formal analysis, Data curation, Conceptualization. **Matteo Morciano:** Writing – review & editing, Supervision, Formal analysis, Data curation. **Elena Campagnoli:** Writing – review & editing, Resources, Investigation. **Valter Giaretto:** Writing – review & editing, Resources, Investigation. **Matteo Fasano:** Writing – review & editing, Supervision, Formal analysis, Data curation. **Eliodoro Chiavazzo:** Writing – review & editing, Supervision, Project administration, Funding acquisition, Conceptualization.

Declaration of competing interest

The authors declare the following financial interests/personal relationships which may be considered as potential competing interests: Eliodoro Chiavazzo reports financial support was provided by Ministero dell'Ambiente e della Sicurezza Energetica (MASE). If there are other authors, they declare that they have no known competing financial interests or personal relationships that could have appeared to influence the work reported in this paper.

Acknowledgments

We acknowledge the financial support of the research contract PTR 2022/24 - ENEA (Studio di sistemi di accumulo termico innovativi basati sull'utilizzo di nano-PCM dinamici: Modellazione e analisi sperimentale delle proprietà termofisiche, realizzazione e testing di un prototipo, e analisi delle possibili applicazioni di tale tecnologia nell'ambito dell'accumulo termico) funded by Ministero dell'Ambiente e della Sicurezza Energetica (MASE) and also thank the Clean Water Center at Politecnico di Torino for the access to OCT facility.

This work has been partly supported by the European Commission in the framework of the project SoFiA—Soap Film based Artificial Photosynthesis—grant agreement 828838.

Data availability

Data will be made available on request.

References

[1] D. Meng, et al., Carboxymethyl cellulose enhanced polymeric form stable phase change materials with reversible transparency for energy storage, ACS Sustain. Chem. \& Eng. 12 (42) (2024) 15623–15633.
[2] J. Li, et al., Effect of twisted fins on the melting performance of PCM in a latent heat thermal energy storage system in vertical and horizontal orientations: energy and exergy analysis, Appl. Therm. Eng. 219 (2023) 119489.
[3] G. Mancardi, et al., A computational view on nanomaterial intrinsic and extrinsic features for nanosafety and sustainability, Mater. Today 67 (2023) 344–370.
[4] Y. Wu, et al., High-efficiency photo-thermo-electric system with waste heat utilization and energy storage, ACS Appl. Mater. \& Interfaces 14 (35) (2022) 40437–40446.
[5] V. V Tyagi, N.A.A. Rahim, N.A. Rahim, A. Jeyraj, L. Selvaraj, Progress in solar PV technology: research and achievement, Renew. Sustain. energy Rev. 20 (2013) 443–461.
[6] V. Chinnasamy, J. Heo, S. Jung, H. Lee, H. Cho, Shape stabilized phase change materials based on different support structures for thermal energy storage applications–A review, Energy 262 (2023) 125463.
[7] S. Wang, et al., Regulating cold energy from the universe by bifunctional phase change materials for sustainable cooling, Adv. Energy Mater. 14 (45) (2024) 2402667.
[8] Y. Li, Y. Fan, Z. Liu, J. Zhang, J. Cheng, Q. Lian, Photo-curable bio-based comb/bottle brush epoxy resin/beeswax/copper foam phase change materials with high enthalpy value, high conductivity, and multifunctional properties, Compos. Sci. Technol. 250 (2024) 110506.
[9] A. Ribezzo, G. Falciani, L. Bergamasco, M. Fasano, E. Chiavazzo, An overview on the use of additives and preparation procedure in phase change materials for thermal energy storage with a focus on long term applications, J. Energy Storage 53 (2022) 105140, https://doi.org/10.1016/j.est.2022.105140. January.
[10] S. Zhao, et al., Elevating the photothermal conversion efficiency of phase-change materials simultaneously toward solar energy storage, self-healing, and recyclability, ACS Appl. Mater. \& Interfaces 14 (25) (2022) 29213–29222.
[11] H. Wang, X. Li, B. Luo, K. Wei, G. Zeng, The MXene/water nanofluids with high stability and photo-thermal conversion for direct absorption solar collectors: a comparative study, Energy 227 (2021) 120483.
[12] S.-Y. Li, T. Yan, Y.-J. Huo, W.-G. Pan, Carbon nanotube/carbon foam thermal-bridge enhancing solar energy conversion and storage of phase change materials, Mater. Today Sustain. 28 (2024) 100986.
[13] J. He, W. Chu, Q. Wang, Experimental study on pressure-enhanced close contact melting with PCMs for stable temperature control of high heat flux electronic devices, Appl. Therm. Eng. 230 (2023) 120707, https://doi.org/10.1016/j.applthermaleng.2023.120707. PA.
[14] X. Zhang, et al., Thermally enhanced flexible phase change materials for thermal energy conversion and management of wearable electronics, Mater. Today Sustain. 28 (2024) 100960.
[15] S. Cheng, X. Guo, W. Cai, Y. Zhang, X. Zhang, Enhanced thermal management in electronic devices through control-oriented structures, J. Mater. Chem. A (2024).
[16] M. Morciano, M. Fasano, E. Chiavazzo, L. Mongibello, Trending applications of phase change materials in sustainable thermal engineering: an up-to-date review, Energy Convers. Manag. X (2025) 100862.
[17] Y. Xu, et al., Bio-based, recyclable, and form-stable thermally conductive phase change composite featuring thermally induced flexibility, ACS Appl. Polym. Mater. 6 (14) (2024) 8671–8678, https://doi.org/10.1021/acsapm.4c01756.
[18] B. Wei, et al., Thermal interface materials: from fundamental research to applications, SusMat 4 (6) (2024) e239.
[19] A.K. Mishra, B.B. Lahiri, J. Philip, Carbon black nano particle loaded lauric acid-based form-stable phase change material with enhanced thermal conductivity and photo-thermal conversion for thermal energy storage, Energy 191 (2020) 116572, https://doi.org/10.1016/j.energy.2019.116572.
[20] A. Ribezzo, et al., Enhancement of heat transfer through the incorporation of copper metal wool in latent heat thermal energy storage systems, Renew. Energy 231 (2024) 120888.
[21] M. Morciano, et al., 3D printed lattice metal structures for enhanced heat transfer in latent heat storage systems, J. Energy Storage 65 (2023) 107350, https://doi.org/10.1016/j.est.2023.107350. September 2022.
[22] R.K. Rajamony, et al., Evaluating the energy and economic performance of hybrid photovoltaic thermal system integrated with multiwalled carbon nanotubes enhanced phase change material, Mater. Today Sustain. 28 (2024) 101035.
[23] Y.A. Bhutto, A.K. Pandey, A. Islam, R.K. Rajamony, R. Saidur, Lauric acid based form-stable phase change material for effective electronic thermal management and energy storage application, Mater. Today Sustain. 28 (2024) 100931.
[24] M.R.Y. McCord, H. Baniasadi, Advancements in form-stabilized phase change materials: stabilization mechanisms, multifunctionalities, and applications-A comprehensive review, Mater. Today Energy (2024) 101532.
[25] K. Liang, L. Shi, J. Zhang, J. Cheng, X. Wang, Fabrication of shape-stable composite phase change materials based on lauric acid and graphene/graphene oxide complex aerogels for enhancement of thermal energy storage and electrical conduction, Thermochim. Acta 664 (2018) 1–15, https://doi.org/10.1016/j.tca.2018.04.002. March.
[26] X. Zuo, et al., Lauric acid/expanded graphite composite phase change film with high thermal conductivity for thermal management, Energy \& Fuels 38 (3) (2024) 2480–2488.
[27] S. Liu, J. Han, L. Wang, Y. Gao, H. Sun, W. Li, A lauric acid-hybridized bentonite composite phase-changing material for thermal energy storage, RSC Adv 10 (43) (2020) 25864–25873.
[28] Y. Ma, et al., EG@ Bi-MOF derived porous carbon/lauric acid composite phase change materials for thermal management of batteries, Energy 272 (2023) 127180.
[29] K. Yu, Y. Liu, M. Jia, Y. Yang, Bio-based dual-functionalized phase change composite: ultrafast solar-to-thermal conversion and reinforced heat storage capacity, Energy and Fuels 35 (19) (2021) 16162–16173, https://doi.org/10.1021/acs.energyfuels.1c02203.
[30] Y. Liu, et al., Flexible phase change composites based on hierarchically porous polypyrrole scaffold for broad-band solar absorption and efficient solar-thermal-electric energy conversion, Compos. Sci. Technol. 250 (2024) 110519.
[31] A. Ribezzo, L. Bergamasco, M. Morciano, M. Fasano, L. Mongibello, E. Chiavazzo, Experimental analysis of carbon-based phase change materials composites for a fast numerical design of cold energy storage systems, Appl. Therm. Eng. 231 (2023) 120907, https://doi.org/10.1016/j.applthermaleng.2023.120907. July 2022.
[32] J. Paul, et al., Nano-enhanced organic form stable PCMs for medium temperature solar thermal energy harvesting: recent progresses, challenges, and opportunities, Renew. Sustain. Energy Rev. 161 (2022) 112321.
[33] L. He, H. Wang, H. Zhu, Y. Gu, X. Li, X. Mao, Thermal properties of PEG/graphene nanoplatelets (GNPs) composite phase change materials with enhanced thermal conductivity and photo-thermal performance, Appl. Sci. 8 (12) (2018) 2613.
[34] A.K. Mishra, B.B. Lahiri, J. Philip, Superior thermal conductivity and photo-thermal conversion efficiency of carbon black loaded organic phase change material, J. Mol. Liq. 285 (2019) 640–657, https://doi.org/10.1016/j.molliq.2019.04.132.
[35] X. Du, J. Xu, S. Deng, Z. Du, X. Cheng, H. Wang, Amino-functionalized single-walled carbon nanotubes-integrated polyurethane phase change composites with superior photothermal conversion efficiency and thermal conductivity, ACS Sustain. Chem. Eng. 7 (21) (2019) 17682–17690, https://doi.org/10.1021/acssuschemeng.9b03853.
[36] R.K. Rajamony, et al., Experimental investigation on the performance of binary carbon-based nano-enhanced inorganic phase change materials for thermal energy storage applications, J. Energy Storage 86 (2024) 111373.
[37] X. Huang, et al., Shape-stabilized phase change materials based on porous supports for thermal energy storage applications, Chem. Eng. J. 356 (2019) 641–661.
[38] N. Jose, M.R. Ravindra, Microencapsulation approaches for the development of novel thermal energy storage systems and their applications, Sol. Energy Mater. Sol. Cells 280 (2025) 113271.
[39] K. Pielichowska, K. Pielichowski, Phase change materials for thermal energy storage, Prog. Mater. Sci. 65 (2014) 67–123.
[40] R. Bidiyasar, R. Kumar, N. Jakhar, A critical review of polymer support-based shape-stabilized phase change materials for thermal energy storage applications, Energy Storage 6 (4) (2024) 1–39, https://doi.org/10.1002/est2.639.
[41] S. Liu, H. Wu, Y. Du, X. Lu, J. Qu, Shape-stable composite phase change materials encapsulated by bio-based balsa wood for thermal energy storage, Sol. Energy Mater. Sol. Cells 230 (2021) 111187.

[42] S. Zhang, et al., A review of phase change heat transfer in shape-stabilized phase change materials (ss-PCMs) based on porous supports for thermal energy storage, Renew. Sustain. Energy Rev. 135 (2021) 110127.

[43] P.K.S. Rathore, S.K. Shukla, Enhanced thermophysical properties of organic PCM through shape stabilization for thermal energy storage in buildings: a state of the art review, Energy Build. 236 (2021) 110799.

[44] D. Das, U. Bordoloi, H.H. Muigai, P. Kalita, A novel form stable PCM based bio composite material for solar thermal energy storage applications, J. Energy Storage 30 (2020) 101403.

[45] N. Gao, et al., Bio-based sunflower carbon/polyethylene glycol shape-stabilized phase change materials for thermal energy storage, RSC Adv 14 (33) (2024) 24141–24151, https://doi.org/10.1039/d4ra03208j.

[46] B. Liu, et al., Research progress of biomass materials in the application of organic phase change energy storage materials, J. Mater. Chem. A 12 (15) (2024) 8663–8682, https://doi.org/10.1039/d3ta07521d.

[47] G. Vasilyev, N. Koifman, M. Shuster, M. Gishvoliner, Y. Cohen, E. Zussman, Phase change material with gelation imparting shape stability, ACS Omega 7 (14) (2022) 11887–11902, https://doi.org/10.1021/acsomega.1c07376.

[48] M. Souissi, A. Trigui, I. Jedidi, M.S. Loukil, M. Abdelmouleh, Bio-based composite as phase change material including spent coffee grounds and beeswax paraffin, Korean J. Chem. Eng. 40 (9) (2023) 2342–2355, https://doi.org/10.1007/s11814-023-1448-5.

[49] X. Hu, H. Huang, Y. Hu, X. Lu, Y. Qin, Novel bio-based composite phase change materials with reduced graphene oxide-functionalized spent coffee grounds for efficient solar-to-thermal energy storage, Sol. Energy Mater. Sol. Cells 219 (2021), https://doi.org/10.1016/j.solmat.2020.110790. July 2020.

[50] M. Daglia, M.T. Cuzzoni, C. Dacarro, Antibacterial activity of coffee, J. Agric. Food Chem. 42 (10) (1994) 2270–2272.

[51] M.S. Mohtasim, B.K. Das, Biomimetic and bio-derived composite phase change materials for thermal energy storage applications: a thorough analysis and future research directions, J. Energy Storage 84 (2024) 110945.

[52] M.R.Y. McCord, J.B. Zimmerman, O.J. Rojas, Harnessing multifunctional electrospun nanofibers containing phase change materials for energy-efficient thermal management: a review on recent trends, Nano Energy (2024) 110212.

[53] M. Zadshir, B.-W. Kim, H. Yin, Bio-based phase change materials for sustainable development, Materials (Basel) 17 (19) (2024) 4816.

[54] B. Teja, et al., Bio-based phase-change materials for thermal energy storage : recent advances, challenges, and outlook, Results Eng 28 (August) (2025) 107087, https://doi.org/10.1016/j.rineng.2025.107087.

[55] C. Wang, C. Cheng, T. Jin, H. Dong, Review on bio-based shape-stable phase change materials for thermal energy storage and utilization, J. Renew. Sustain. Energy 14 (5) (2022).

[56] D. Huang, Z. Wang, X. Sheng, Y. Chen, Bio-based MXene hybrid aerogel/paraffin composite phase change materials with superior photo and electrical responses toward solar thermal energy storage, Sol. Energy Mater. Sol. Cells 251 (2023) 112124.

[57] A. Palacios, L. Cong, M.E. Navarro, Y. Ding, C. Barreneche, Thermal conductivity measurement techniques for characterizing thermal energy storage materials – a review, Renew. Sustain. Energy Rev. 108 (March) (2019) 32–52, https://doi.org/10.1016/j.rser.2019.03.020.

[58] Z. Chen, F. Shan, L. Cao, G. Fang, Synthesis and thermal properties of shape-stabilized lauric acid/activated carbon composites as phase change materials for thermal energy storage, Sol. Energy Mater. Sol. Cells 102 (2012) 131–136, https://doi.org/10.1016/j.solmat.2012.03.013.

[59] G. Zhang, Y. Sun, C. Wu, X. Yan, W. Zhao, C. Peng, Low-cost and highly thermally conductive lauric acid–paraffin–expanded graphite multifunctional composite phase change materials for quenching thermal runaway of lithium-ion battery, Energy Reports 9 (2023) 2538–2547, https://doi.org/10.1016/j.egyr.2023.01.102.

[60] W. Wang, T. Fu, G. Fang, Preparation and thermal performances of lauric acid/polyvinyl butyral/graphene nanoplates composite phase change materials, Phys. status solidi 221 (10) (2024) 2400104.

[61] C. Yanghua, L.I.U. Yuan, W. Zhaohe, Preparation and characteristics of microencapsulated lauric acid as composite thermal energy storage materials, Mater. Sci. 26 (1) (2020) 88–93.

[62] X. Liu, A. Fleischer, G. Feng, Nanoencapsulated lauric acid with a poly (Methyl methacrylate) shell for thermal energy storage with optimum capacity and reliability, ACS Appl. Polym. Mater. 3 (5) (2021) 2341–2351.

[63] R.M. Saeed, J.P. Schlegel, C. Castano, R. Sawafta, V. Kuturu, Preparation and thermal performance of methyl palmitate and lauric acid eutectic mixture as phase change material (PCM), J. Energy Storage 13 (2017) 418–424, https://doi.org/10.1016/j.est.2017.08.005.

[64] J. Sobczak, et al., Thermophysical profile of ethylene glycol based nanofluids containing two types of carbon Black nanoparticles with different specific surface areas, J. Mol. Liq. 326 (2021) 115255.

[65] H. Waqas, et al., Enhancing the performance of thermal energy storage by adding nano-particles with paraffin phase change materials, Nanotechnol. Rev. 13 (1) (2024) 20230180.

[66] A.Y.C. Delgado, H.J.C. Velásquez, D.A.R. Molina, Thermal and thermodynamic characterization of a dye powder from liquid turmeric extracts by spray drying, Rev. Fac. Nac. Agron. Medell{\'\i}n 69 (1) (2016) 7845–7854.

[67] P.C. Singh, R.K. Singh, S. Bhamidipati, S.N. Singh, P. Barone, Thermophysical properties of fresh and roasted coffee powders 1, J. Food Process Eng. 20 (1) (1997) 31–50.

[68] P. Makishi, Y. Shimada, A. Sadr, J. Tagami, Y. Sumi, Non-destructive 3D imaging of composite restorations using optical coherence tomography: marginal adaptation of self-etch adhesives, J. Dent. 39 (4) (2011) 316–325.

[69] P. Liu, R.M. Groves, R. Benedictus, Optical coherence tomography for the study of polymer and polymer matrix composites, Strain 50 (5) (2014) 436–443.

[70] V. Tropsa, A. Ivankovic, J.G. Williams, Predicting residual stresses due to solidification in cast plastic plates, Plast. rubber Compos. 29 (9) (2000) 468–474.

[71] A.K. Mishra, B.B. Lahiri, V. Solomon, J. Philip, Nano-inclusion aided thermal conductivity enhancement in palmitic acid/di-methyl formamide phase change material for latent heat thermal energy storage, Thermochim. Acta 678 (June) (2019) 178309, https://doi.org/10.1016/j.tca.2019.178309.

[72] A.K. Mishra, B.B. Lahiri, J. Philip, Thermal conductivity enhancement in organic phase change material (phenol-water system) upon addition of Al2O3, SiO2 and TiO2 nano-inclusions, J. Mol. Liq. 269 (2018) 47–63, https://doi.org/10.1016/j.molliq.2018.08.001.

[73] T. Nomura, K. Tabuchi, C. Zhu, N. Sheng, S. Wang, T. Akiyama, High thermal conductivity phase change composite with percolating carbon fiber network, Appl. Energy 154 (2015) 678–685.

[74] R. Zheng, J. Gao, J. Wang, G. Chen, Reversible temperature regulation of electrical and thermal conductivity using liquid–solid phase transitions, Nat. Commun. 2 (1) (2011) 289.

[75] S. Harish, D. Orejon, Y. Takata, M. Kohno, Thermal conductivity enhancement of lauric acid phase change nanocomposite with graphene nanoplatelets, Appl. Therm. Eng. 80 (2015) 205–211, https://doi.org/10.1016/j.applthermaleng.2015.01.056.

[76] N. Radhakrishnan, C.B. Sobhan, Thermophysical characterization and melting heat transfer analysis of an organic phase change material dispersed with GNP-Ag hybrid nanoparticles, Heat Mass Transf. und Stoffuebertragung 58 (10) (2022) 1811–1828, https://doi.org/10.1007/s00231-022-03218-x.

[77] Y. Wu, X. Yan, P. Meng, P. Sun, G. Cheng, R. Zheng, Carbon black/octadecane composites for room temperature electrical and thermal regulation, Carbon N. Y. 94 (2015) 417–423.

[78] D.B. Cardoso, E.T. de Andrade, R.A. Aragón Calderón, M.H.S. Rabelo, C. de A. Dias, I.Á. Lemos, Determination of thermal properties of coffee beans at different degrees of roasting, Coffee Science 13 (4) (2018) 498–509.

[79] G. Jeevarathinam, T. Pandiarajan, Thermal properties of turmeric rhizomes, Adv. Life Sci. 5 (12) (2016) 5167–5170.

[80] R.K. Rajamony, et al., Eco-friendly approach to thermal energy storage: assessing the thermal and chemical properties of coconut biochar-enhanced phase change material, Energy Storage 6 (5) (2024) e679.

[81] C. Shi, et al., Large-scale production of spent coffee ground-based photothermal materials for high-efficiency solar-driven interfacial evaporation, Chem. Eng. J. 455 (2023) 1–9, https://doi.org/10.1016/j.cej.2022.140361. September 2022.

[82] J. Yang, et al., Exploring the properties and potential uses of biocarbon from spent coffee grounds: a comparative look at dry and wet processing methods, Processes 11 (7) (2023) 2099.

[83] D. Kuttigounder, J.R. Lingamallu, S. Bhattacharya, Turmeric powder and starch: selected physical, physicochemical, and microstructural properties, J. Food Sci. 76 (9) (2011). C1284–C1291.

[84] L. Zhou, L.-S. Tang, X.-F. Tao, J. Yang, M.-B. Yang, W. Yang, Facile fabrication of shape-stabilized polyethylene glycol/cellulose nanocrystal phase change materials based on thiol-ene click chemistry and solvent exchange, Chem. Eng. J. 396 (2020) 125206.

[85] Z. Zhang, et al., Carbon-intercalated halloysite-based aerogel efficiently encapsulating phase change materials with excellent photothermal conversion and energy storage, Chem. Eng. J. 498 (2024) 155279.

[86] L. Li, J. Song, Y. Wang, M. Du, Q. Wei, Y. Cai, Fabrication and performance of shape-stable phase change composites supported by environment-friendly and economical loofah sponge fibers for thermal energy storage, Energy \& Fuels 36 (7) (2022) 3938–3946.

[87] X. Cui, et al., Photothermal nanomaterials: a powerful light-to-heat converter, Chem. Rev. 123 (11) (2023) 6891–6952, https://doi.org/10.1021/acs.chemrev.3c00159.

[88] Y. Wang, B. Tang, S. Zhang, Single-walled carbon nanotube/phase change material composites: sunlight-driven, reversible, form-stable phase transitions for solar thermal energy storage, Adv. Funct. Mater. 23 (35) (2013) 4354–4360, https://doi.org/10.1002/adfm.201203728.

[89] Z. Cai, et al., Flexible phase change materials with enhanced tensile strength, thermal conductivity and photo-thermal performance, Sol. Energy Mater. Sol. Cells 219 (2021) 1–7, https://doi.org/10.1016/j.solmat.2020.110728. July 2020.

[90] W. Dong, et al., Coffee grounds-based hydrogel as a high-performance and durable evaporator for solar-driven freshwater generation, Mater. Today Energy 30 (2022) 101187.

[91] X. Hu, H. Huang, Y. Hu, X. Lu, Y. Qin, Novel bio-based composite phase change materials with reduced graphene oxide-functionalized spent coffee grounds for efficient solar-to-thermal energy storage, Sol. Energy Mater. Sol. Cells 219 (2021) 110790.

[92] M. Alberghini, et al., Coffee-based colloids for direct solar absorption, Sci. Rep. 9 (1) (2019) 1–11, https://doi.org/10.1038/s41598-019-39032-5.

[93] S.R. Deka, S. Yadav, D. Kumar, S. Garg, M. Mahato, A.K. Sharma, Self-assembled dehydropeptide nano carriers for delivery of ornidazole and curcumin, Colloids Surfaces B Biointerfaces 155 (2017) 332–340.

[94] J.Y. Kim, Y.Y. Kang, E.J. Kim, J.-H. Ahn, H. Mok, Effects of curcumin-/boron-based compound complexation on antioxidant and antiproliferation activity, Appl. Biol. Chem. 61 (2018) 403–408.

[95] J. Chen, et al., Highly stable MXene-based phase change composites with enhanced thermal conductivity and photothermal storage capability, ACS Appl. Energy Mater. 5 (9) (2022) 11669–11683.
[96] L. Yang, Y. Yuan, N. Zhang, Y. Dong, Y. Sun, W. Ji, Photo-to-thermal conversion and energy storage of lauric acid/expanded graphite composite phase change materials, Int. J. Energy Res. 44 (11) (2020) 8555–8566.
[97] W. Tian, Y. Xiao, G. Qin, X. Zheng, Anisotropic and shape-stable sugarcane-based phase change composites in the application of solar thermal energy storage, Energy 308 (2024) 132942.
[98] K.K. Gupta, P.K.S. Rathore, B.S. Sikarwar, A.K. Pandey, Solar to thermal energy storage performance of composite phase change material supported by copper foam loaded with graphite and boron nitride, Sol. Energy 272 (2024) 112459.
[99] Y. Xie, et al., MXene-modified bio-based pitaya peel foam/polyethylene glycol composite phase change material with excellent photo-thermal conversion efficiency, thermal energy storage capacity and thermal conductivity, J. Energy Storage 78 (2024) 110089.
[100] M. Li, C. Wang, Preparation and characterization of GO/PEG photo-thermal conversion form-stable composite phase change materials, Renew. Energy 141 (2019) 1005–1012.
[101] X. Zou, J. Liu, Polyoxyethylene based phase change materials with enhanced mechanical property, thermal conductivity and photo-thermal energy charging capacity, Energy Reports 6 (2020) 2948–2955.
[102] X. Pan, N. Zhang, Y. Yuan, X. Shao, W. Zhong, L. Yang, Balsa-based porous carbon composite phase change material with photo-thermal conversion performance for thermal energy storage, Sol. Energy 230 (2021) 269–277.
[103] S. Liu, et al., Effects of biochar pyrolysis temperature on thermal properties of polyethylene glycol/biochar composites as shape-stable biocomposite phase change materials, RSC Adv. 12 (16) (2022) 9587–9598.
[104] H. Faraji, Ç. Y\ild\iz, A. Arshad, M. Ar\ic\i, K. Choukairy, M. El Alami, Passive thermal management strategy for cooling multiple portable electronic components: hybrid nanoparticles enhanced phase change materials as an innovative solution, J. Energy Storage 70 (2023) 108087.
[105] A.K. Mishra, et al., Dynamic PCM strategies with nano-enhanced composites for optimal thermal energy storage and management, Chem. Eng. J. Adv. 23 (June) (2025) 100789, https://doi.org/10.1016/j.ceja.2025.100789.
[106] Y. Jing, Z. Zhao, X. Cao, Q. Sun, Y. Yuan, T. Li, Ultraflexible, cost-effective and scalable polymer-based phase change composites via chemical cross-linking for wearable thermal management, Nat. Commun. 14 (1) (2023) 8060.
[107] S. Cai, et al., Development of bio-based flexible phase change materials utilizing lauric acid for battery thermal management systems, J. Energy Storage 86 (February) (2024), https://doi.org/10.1016/j.est.2024.111382.
[108] Y. Su, et al., Bio-based eutectic composite phase change materials with enhanced thermal conductivity and excellent shape stabilization for battery thermal management, J. Energy Storage 100 (2024) 113712.
[109] W. Wu, W. Wu, S. Wang, Thermal management optimization of a prismatic battery with shape-stabilized phase change material, Int. J. Heat Mass Transf. 121 (2018) 967–977.